Temperature-Dependent Photonic Bandgap in a Self-Assembled Hydrogen-Bonded Liquid-Crystalline Diblock Copolymer**

By *Chinedum Osuji*, *Chi-Yang Chao*, *Ion Bita*, *Christopher K. Ober*, and *Edwin L. Thomas**

We take advantage of self-assembly in a hierarchically structured, hybrid material to develop photonic bandgaps in the visible which may be systematically tuned by application of thermal or electric fields. Hydrogen bonding between a host polymer and a guest small molecule is used to augment the molecular weight of an appropriately selected coil–coil diblock copolymer to bring the microdomain structure onto the length scale needed for significant interaction with visible light. Further, the use of liquid-crystal-mesophase-forming moieties as the guest hydrogen-bonding units adds functionality to the system as the optical properties of the liquid-crystalline domains can be modulated by external stimuli. We use hydrogen bonding to sequester varying amounts of imidazole terminated mesogens within the acid domains of a poly[styrene-*block*-poly-(methacrylic acid)] (PS-*b*-MAA) diblock copolymer. The resulting PS-*b*-MAA/LC side-group liquid-crystalline diblock copolymer possesses a photonic bandgap in the green with the exact location and structure of the gap dependent on the composition of the system. Here, we discuss the structure and optical properties of these materials as a function of their composition and the response of the optical properties to temperature. Varying the order parameter of the LC domains by heating into the isotropic state changes the peak reflectivity by 40 nm, resulting in a color change from green to orange.

1. Introduction

Photonic crystals have received much attention as they offer new ways to transport and manipulate information optically. Researchers have fabricated many types of photonic crystals and begun their integration into optical systems. One, two, and three dimensionally periodic photonic crystals have been constructed using a variety of methods: by conventional photolithography,[1] holography,[2] by sequential deposition of alternating layers (thermal evaporation, sputtering, solvent spinning, polyelectrolyte adsorption),[3] by self-assembly of colloidal crystals,[4–10] by self-assembly of block copolymers,[11–14] and by polymer multilayer co-extrusion.[15] The self-assembly approach is attractive as it offers a low-cost method for the production of photonic crystals using both organic and inorganic components. One drawback to self-assembly is the limited number of structures and symmetries currently accessible, although considerable effort in supramolecular self-assembly continues to introduce new structures at a rapid pace.[16]

The use of various types of building blocks and the interplay of the ordering tendencies of the constituent blocks in hierarchically ordered materials affords some extra degrees of freedom to the polymer scientist in the design of self-assembling systems.[17] Hydrogen bonding is ubiquitous in nature as the modest "glue" that helps bind and build small moieties into supramolecular assemblies with dimensions that may extend to the micrometer scale. Biomimetic approaches to materials synthesis can also introduce new structures such as hybrid organic–inorganic material systems with good dielectric contrast. In addition to the need to provide a large difference in the respective dielectric constants of the materials comprising the photonic crystal, it is highly desirable to utilize materials whose index of refraction may be tailored and thus afford tunable photonic crystals. Several approaches to tunability have been explored; one route is to use optical pumping to create free charge carriers in a semiconductor,[18] another is to trigger a change in the lattice spacing of a colloidal crystal gel by for example, pH, temperature, ionic strength etc.,[4,5] another is to mechanically deform the lattice,[12] and another is to infiltrate the photonic crystal with a liquid crystal.[19–22]

The use of hydrogen bonds to attach small molecules including mesogenic species to host homopolymer backbones is well documented.[23] We have used hydrogen bonding to deliberately induce the formation of a liquid-crystalline mesophase in one block of a suitable coil–coil diblock copolymer host. The incorporation of liquid crystallinity in a block copolymer results in an active material that can be used in electro-optic devices. For example, our team has explored microphase stabilized ferroelectric liquid-crystalline diblock copolymers for display applications.[24] We report here on the synthesis, by anionic polymerization and hydrogen bonding, of a side group liquid-crystalline diblock copolymer (LC-BCP) with a temperature-

[*]   Prof. E. L. Thomas, C. Osuji, I. Bita
       Program in Polymer Science and Technology
       Department of Materials Science and Engineering
       Massachusetts Institute of Technology
       Cambridge MA 02139 (USA)
       E-mail: elt@mit.edu
       C.-Y. Chao, Prof. C. K. Ober
       Department of Materials Science and Engineering
       Cornell University
       Ithaca NY 14850 (USA)

dependent, limited photonic bandgap in the visible. A polystyrene-*block*-poly(methacrylicacid) (PS-*b*-MAA) block copolymer was anionically synthesized and then imidazole-terminated mesogens were selectively sequestered into the methacrylic acid block via hydrogen bonding with the hydroxy group, thus simultaneously augmenting the molecular weight of, and adding mesogenic function to the block copolymer. We demonstrate that PS-*b*-MAA/LC can self-assemble by simple solvent casting into a one-dimensional (1D) lamellar microdromain structure with a 175 nm period. The as formed structure exhibits an optical stop band in the green. Tunability of this structure is then shown by thermally inducing changes in the refractive index of the LC layers via alteration of the order parameter of the mesogens. The center of the stop band can be reversibly red-shifted by approximately 10 nm for a change of 50 °C.

Both heat and electric fields can be used to dynamically manipulate the index contrast presented to incident polarized light by a periodic LC-BCP photonic crystal. For initial work, we chose the simplest microdomain structure, namely the 1D periodic lamellar structure with alternating layers in our case of polystyrene and poly(methacrylic acid-LC) (PMMA-LC), with the LC-containing layers displaying a smectic structure with homeotropic boundary condition as depicted schematically in structure I of Figure 1a. Polystyrene is isotropic with an index in the visible of 1.59, PMMA is also isotropic with an index of 1.45 and the imidazole mesogen is assumed to be uniaxial with an index of 1.80 in the isotropic regime. The index of refraction of the mesogen was obtained using an effective medium approach. The index of a 0.60 molar ratio blend of the mesogen and poly(methacrylic acid) was measured in the isotropic regime. The measured value is a volume weighted average of the dielectric constants of the mesogen and the polymer, thus yielding the average effective dielectric constant and so the index of refraction of the mesogen since the values for the poly(methacrylic acid) are known.

Thus, at temperatures below the smectic to isotropic transition, light incident along z, polarized along x, experiences an index of $n_A = n_{PS}$ in the polystyrene layers and $n_B = (\varphi_{LC} n_0^2 + (1-\varphi_{LC})n_{PMMA}^2)^{1/2}$ in the PMMA-LC layers where n_{PMAA} is the index of the poly(methacrylic acid) backbone and n_0 is the ordinary refractive index of the mesogens, that is along the x and y axes. When the sample is heated, the indices and layer thicknesses will change depending on the sample density, thermal expansion coefficient, and the orientational order parameter of the mesogens. On thermal clearing of the LC, the sample will have morphology as depicted in structure IIa. In this case, the refractive indices presented to the light are now $n_A' = n_{PS} + \frac{dn}{dT_{PS}} \Delta T$

and $n_B' = (\varphi_{mesogen}\langle n_{mesogen}\rangle^2 + (1 - \varphi_{LC})n_{PMMA}^2)^{1/2} + \frac{dn_{eff}}{dT}\Delta T$

where $\langle n_{mesogen}\rangle$ is the average index for the mesogen given by $\langle n_{mesogen}\rangle = (\frac{2n_o^2+n_e^2}{3})^{1/2}$. For reasonable values of birefringence for the organic mesogen, $\Delta n = n_e - n_0 \sim 0.07$–$0.20$, we can expect a change in the index of B layers in the system upon thermal clearing of the liquid-crystalline state of roughly $\Delta n_B = n_B' - n_B \sim 0.02$–$0.05$ for $\varphi_{mesogen} \sim 0.7$–$0.8$. Calculations using the Berreman transfer matrix method[25] for a 50 bi-layer stack predict
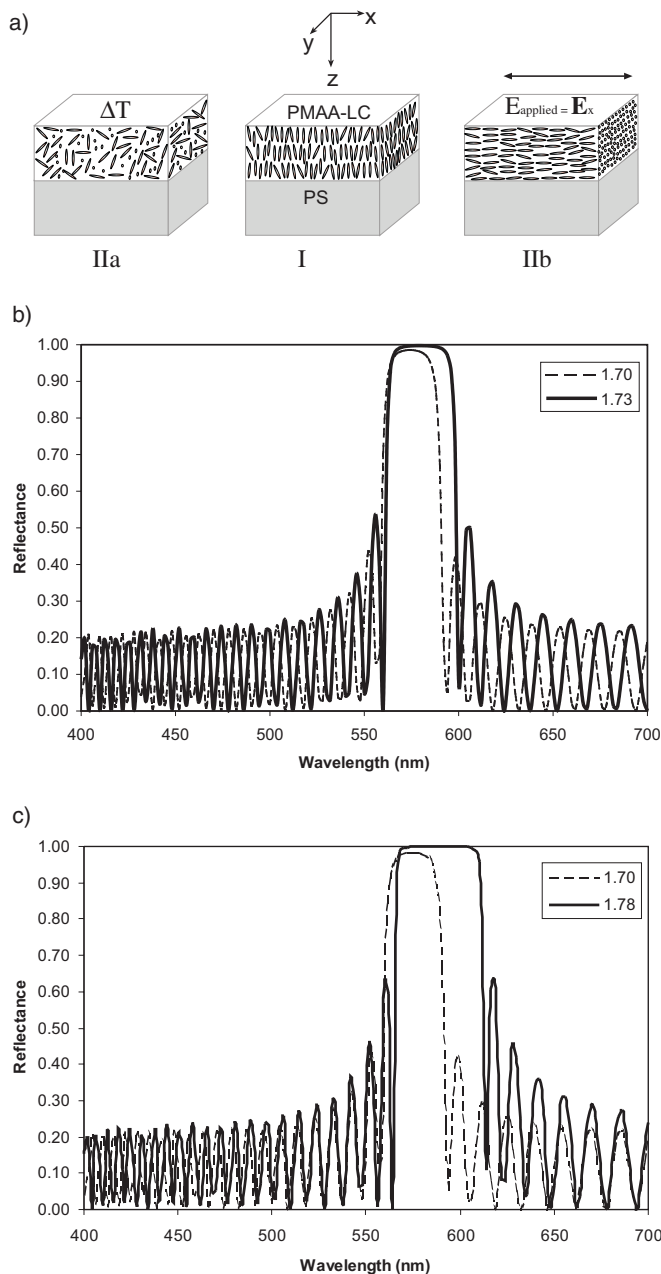

Fig. 1. a) Schematic view of one repeat unit in the 1D self-assembled photonic bandgap material. The material starts off with the LC layers parallel to the lamellae and perpendicular to the propagation direction z. The optical properties of the state I can be changed either by a change of temperature or the application of an electric field, leading to the new states IIa and IIb respectively. On heating through some ΔT, the mesogen orientation randomizes or an electric field, E_x, is used to reorient the LC layers parallel to the x-axis. Simulation of the normal incidence reflectivity from 50 bi-layers with a period of 175 nm. $n_{PS} = 1.59$ and $n_{PMAA-LC} = 1.70$ in the original state I. $\Delta n = n_e - n_0 = 0.10$ for the mesogen, leading to $\Delta n_{PMAA-LC} = 1.78$–$1.70 = 0.08$ for the PMAA-LC domain as a whole. b) Thermal randomization increases the effective $n_{PMAA-LC}$ to 1.73 in state IIa due to contributions from n_e. c) Electric field reorientation of the LC layers increases the effective $n_{PMAA-LC}$ to 1.78 in IIb due to contributions from n_e.

a broadening and shifting of the stop-band towards the red with a corresponding increase in the reflectivity for a temperature above the LC isotropization temperature as shown in Figure 1b.

Alternatively, the index can be changed via an applied electric field to exploit the birefringence of the mesogen in a more direct fashion by reversibly aligning either the ordinary or extraordinary components of the mesogen's refractive index parallel to the oscillation of the electric field of the incoming light. As shown in structure IIb, assuming a positive dielectric susceptibility, an applied electric field E_x realigns the mesogens along the *x*-axis so that for incoming light with electric field vector oscillating along *x*, the index in the B layers is now given by $n''_B = (\varphi_{mesogen}n_e^2 + (1-\varphi_{LC})n_{PMMA}^2)_{1/2}$. In this case, a greater effect is produced, $\Delta n_B = n'_B \sim 0.06$–$0.16$, using the same range of values for the mesogen birefringence (Δn) and volume fraction ($\varphi_{mesogen}$) given above. Light polarized along the *y*-axis (TE) would not be affected by the change in orientation of the mesogen. The effect of the electric field is qualitatively the same as for the thermal case, but much stronger, as shown by the simulation results of Figure 1c. The typically high electric fields (30–300 V/μm) necessary for LC reorientation are usually realized with reasonable voltages by using a thin sample. However, the inherently layered geometry with homeotropic anchoring of the mesogens in our present material requires that a potential difference be placed across the usually large sample dimension along the *x*-direction. In our initial experimental work, we have pursued the thermal approach to index manipulation and are currently working on the electric field method.

2. Results and Discussion

The materials employed are outlined in Figure 2. The neat diblock copolymer, PS-*b*-MAA forms hexagonally packed cylinders of poly(methacrylic acid) embedded in a polystyrene matrix, as deduced by transmission electron microscopy, (TEM) and small-angle X-ray scattering (SAXS). The average cylinder–cylinder spacing was 120 nm and simple cast films of the polymer are clear and colorless. The mesogen is a white powder with a melting point of 46 °C. It is modeled at approximately 30 Å in length and found by SAXS to have a layer period of 54 Å, suggesting a partially interdigitated bilayer arrangement.

When complexed with the mesogen, PS-*b*-MAA formed homogeneous films over the composition range studied, from 0.10 to 0.80 molar ratio of mesogen to acrylic acid repeat units.
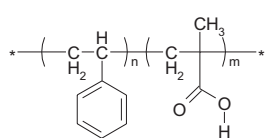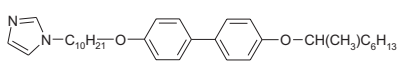
Material	Structure	MW (kg/mol)
Polymer P(S-*b*-MAA)		500-96
LC mesogen Chiral-racemic		0.504

Fig. 2. Structure and molecular weights of host polymer and hydrogen bonding mesogens.

The films did not contain domains of pure mesogen macrophase separated from the block copolymer, as judged by the TEM images as well as absence of the pure mesogen melting peaks in differential scanning calorimetry (DSC) and SAXS. SAXS and DSC also confirmed the formation of a liquid-crystalline phase within the block copolymer that exhibited distinctive structural and thermal characteristics as compared to those of the pure mesogen. Figure 3 shows that the smectic-to-isotropic transition in the LC-BCP occurs over a broad temperature range, from about 65–85 °C. The heat of transition (normalized
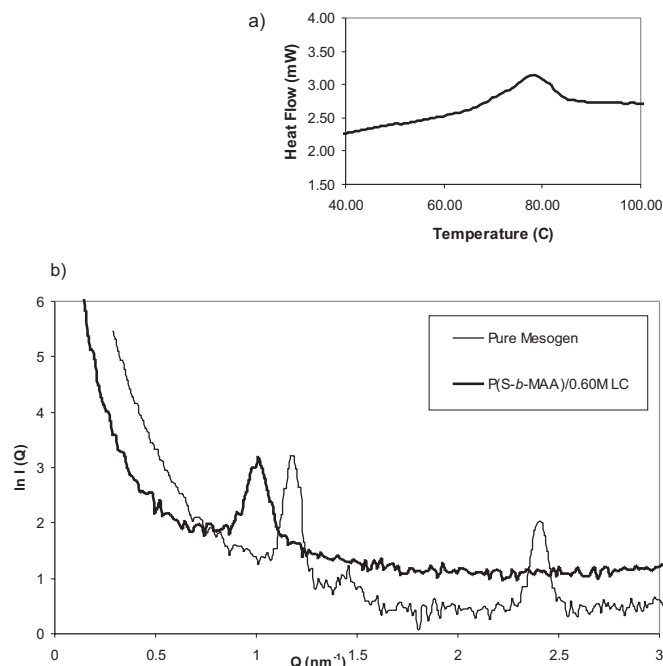

Fig. 3. a) DSC results from PS-*b*-MAA/0.60 M LC and pure mesogen. A heating rate of 10 °C/min was used. b) SAXS from PS-*b*-MAA/0.60 M LC and the pure mesogen.

to the LC block content) on the initial heating is 10.7 J/g whereas it is 3.2 J/g on second and subsequent heatings. The disparity in the enthalpies suggests that the first passage through the clearing point involves a transition from an LC structure with a higher degree of order as compared to the second and subsequent transitions. It is possible that the morphology which is initially established during solvent removal becomes inaccessible to the system during the subsequent thermal cycles in the melt state. The transition enthalpy of 3.2 J/g is on the same order of magnitude as observed in covalently bound systems previously studied.[26] Thermal treatments below about 110 °C do not appear to cause substantial amounts of macrophase separation of the mesogen from the block copolymer host—there is no evidence of pure mesogen signatures in the DSC and SAXS of samples which have undergone heating up to 110 °C for short times. Beyond 110 °C, accelerating anhydride formation along the methacrylic acid backbone depletes mesogens from the polymer resulting in their macrophase separation from the polymer chain and the production of turbidity in the films.

PS-*b*-MAA-LC films less than 200 μm thick were clear and appeared blue to green depending on the particular LC content and the viewing angle. In particular, at 0.60 molar ratio (0.60 M) and for normal incidence, green films were produced, as shown in the photograph in Figure 4a. Heating into the isotropic regime gives a film with red-orange color in reflection (Fig. 4b). Bright-field TEM images of cross-sections of the films (Fig. 5) indicate that the LC-BCP self-assembled into a lamellar structure, with a layer period of approximately
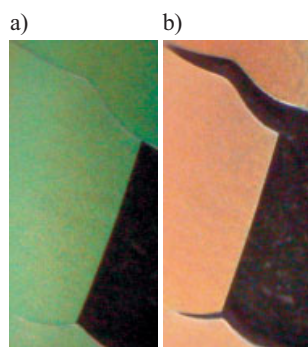
a)   b)

Fig. 4. Photographs of pieces of the reflective polymer, field of view is 1 × 2 mm. The cracks were accidentally introduced during sample removal. a) Sample at 30 °C. b) Sample at 80 °C.
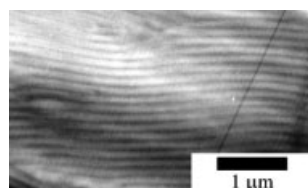
Fig. 5. Transmission electron micrograph from PS-*b*-MAA/0.60 M LC. The dark areas correspond to the MAA-LC domains.

165 nm with the lamellae preferentially oriented parallel to the surface of the glass vial in which the samples were cast. The dark areas in the unstained TEM image correspond to more electron-dense PMMA-LC domains.

SAXS patterns obtained with X-rays incident parallel to the film surface (cross-sectional) confirm the layering of the domains parallel to the substrate surface with quite long range order (Fig. 6). A lamellar period of 175 nm is calculated using the third and higher orders of the lamellar reflections, and is in good agreement with the period derived by the TEM inspec-
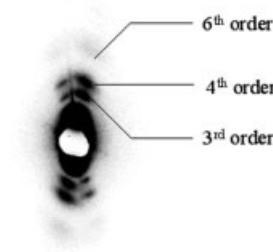
6th order

4th order

3rd order

Fig. 6. Cross-sectional SAXS of PS-*b*-MAA/0.60 M LC. The azimuthal intensity distribution of the third order of the lamellar reflections is used to compute the order parameter of the lamellae.

tion. Order parameters ($P_2 = \langle 3\cos^2\alpha - 1\rangle/2$, the second coefficient of the orientation distribution function) as high as 0.77 for the lamellae and 0.55 for the smectic layers were derived in the manner of Mitchell and Windle[27] from data taken from a particularly well-aligned and large-grained sample. The smectic order parameter was measured as a function of temperature. Starting from 0.29 at 40 °C, it decreased and increased reversibly by a factor of 2 on thermal cycling to 70 °C and back to 40 °C.

We investigated the temperature-dependence of the optical properties of this self-assembled dielectric stack by obtaining the normal incidence transmission spectrum of 200 micrometer thick samples illuminated with an incandescent white light source through a plane polarizer using a hot stage mounted in an optical microscope. A heating and cooling rate of 10 °C/min. was applied. Heating from room temperature (RT) up into, but not beyond the transition region gave a reversible red shift of the minimum of the sample transmittance. In one case, a 9 nm shift from 560 nm to 569 nm occurs over the interval from 40 °C to 70 °C, accompanied by a decrease in the transmitted intensity from about 72 % to 60 %, i.e., the sample became more reflective. Heating beyond the smectic to isotropic transition, to 90 °C, produces a further red shift of 40 nm in the minimum of the sample transmittance without much further change in the magnitude of the transmittance. However these effects are no longer reversible—cooling back to 40 °C from 90 °C recovered the transmission to almost its original value at 72 %, but the minimum remained centered at 600 nm (vs. the 560 nm initial position). Investigations of a broader set of samples revealed this behavior to be quite general. There are two distinct regions, separated by the smectic-isotropic transition, within which the samples exhibit reversibility of both the stop band position and reflective efficiency. This is shown in the data of Figure 7a, where the change from regime I to regime II is well illustrated. We find that after an initial heating above the clearing temperature of the LC, there is a red shift of roughly 0.15 nm/°C and a change in transmitted intensity of -0.2 percentage points per °C, on subsequent heating and cooling cycles between 30 and 90 °C, as shown in the data of Figure 7.

The simulated normal incidence reflectance for three ideal structural states (I, IIa, IIb) is plotted in Figures 1b and c. Since experimental samples exhibit layer misorientation as well as a relatively low and a temperature-dependent order parameter of the mesogens, it is informative to compute the reflectance as a function of incident angle for TE and TM polarizations for suitable choices of refractive indices. Figure 8 shows the reflectance calculated using 50 periods for various mesogen orientations. Particularly interesting is the case in which the index of the PS domain is matched by that of the extraordinary component of the PMAA-LC domain. It results in the functioning of the material as a polarizing filter, as TE modes within the bandgap are stopped whilst TM modes are allowed to propagate. From simulations such as these, we are able to identify relevant criteria (refractive indices, mesogen orientation, anchoring conditions, and microdomain geometry) that we can use in the design of our material system to achieve particular properties.
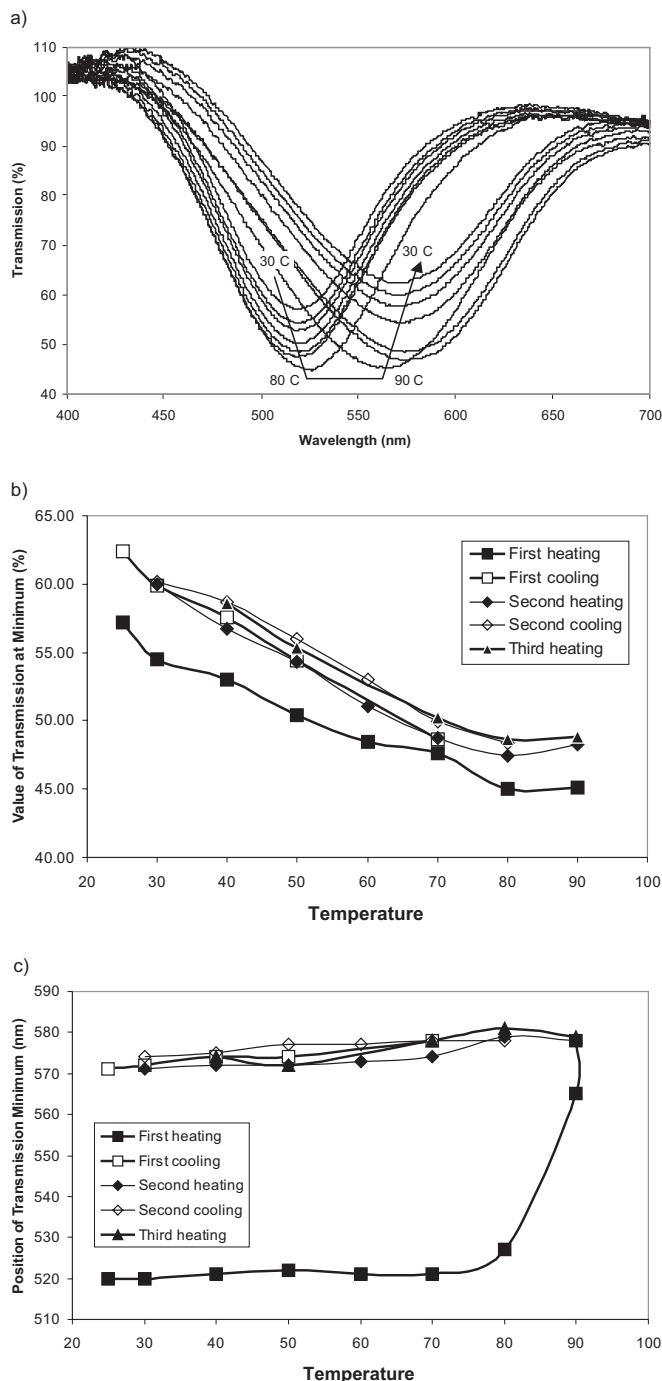
FULL PAPER

a)

b)

c)

Fig. 7. a) Transmission as a function of temperature. The sample is heated continuously from 30 °C to 90 °C and then cooled back to 30 °C. b) Minimum transmission as a function of temperature. c) Location of stop band minimum as a function of temperature.

Fig. 8. Calculated reflectance as a function of angle for TE and TM polarizations using 50 periods with $d_{PMAA-LC} = 75$ nm and $d_{PS} = 85$ nm. The plane of incidence is the xz plane, as in Figure 1. Angles are in degrees off-normal. Case I: $n_{PS} = 1.590$, $n_{PMAA} = 1.450$, $n_e = 1.866$, $n_0 = 1.766$, and $\varphi_{mesogen} = 0.783$. Thus for the medium PMAA-LC, $\Delta n_{PMAA-LC} = 1.78\text{-}1.70 = 0.08$. a) Mesogen optical axis is along the z direction. b) Mesogen optical axis is along the x direction. c) Mesogen optical axis is along the y direction. Case II: $n_{PS} = 1.590$, $n_{PMAA} = 1.450$, $n_e = 1.630$, $n_0 = 1.430$, and $\varphi_{mesogen} = 0.783$. Thus for the medium PMAA-LC, $\Delta n_{PMAA-LC} = 1.593\text{-}1.434 = 0.159$. The interesting case of index matching between the PS domains and the extraordinary component of the PMAA-LC effective medium makes the medium a polarizing filter as TE modes within the bandgap are rejected whilst TM modes pass through as in b, or the reverse as in c. With the optical axis along z, the symmetry between TE and TM at normal incidence returns, as expected. a) Mesogen optical axis is along the z-direction. b) Mesogen optical axis is along the x direction. c) Mesogen optical axis is along the y direction.

between the layers that we would expect given the morphology of our material and the geometry of the experiment. We interpret the gradual change in transmission as due to a similarly gradual, rather than sharp, transition in the order parameter of the mesogens on melting. The small, broad second heating transition centered at 78 °C and the lack of an observable exotherm on cooling suggest that the packing of the mesogens in the original "as-cast" state is quite different than in states achieved by subsequent thermal cycling of the material. The significant rate dependence of the enthalpy of the transition—e.g., cooling faster than 20 °C/min. in the DSC resulted in the absence of the peak in a subsequent heating experiment, also suggests that the reorganization of the mesogens is relatively slow. It is very likely that the morphology space accessible to the sample in the solid state is very different than that it experienced in the presence of solvent, such as when initially produced by casting. Path dependent morphologies are an important feature of liquid-crystalline block copolymers.[26]

Our experimental results are well in line with those predicted by our simulations. That is, there is an increase in the efficiency of the stop band as observed by the deepening of the transmission dip, and a small shift of the stop band to higher wavelengths. This is congruent with the increase in index contrast
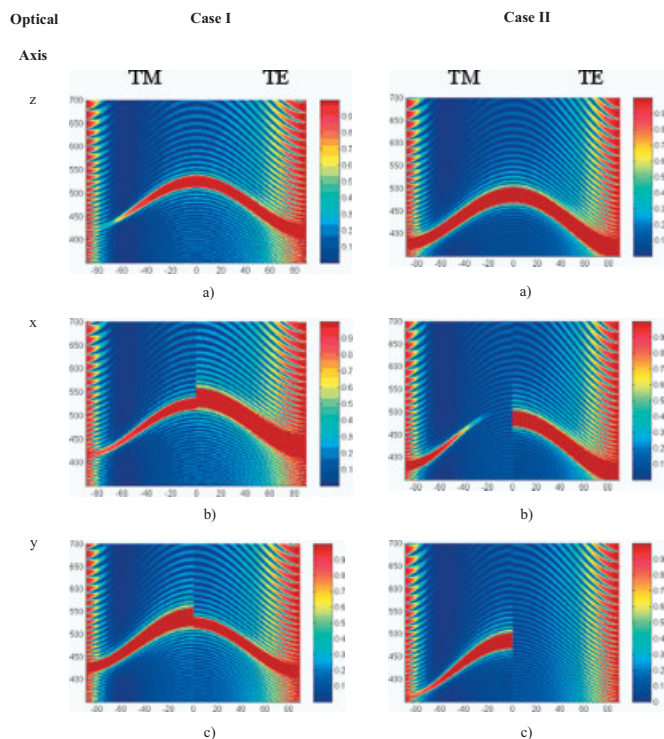
3. Conclusion

In summary, we have shown that very interesting optical properties can be achieved in even simple 1D periodic systems by employing birefringent media, as has recently been demonstrated in the case the multilayer films produced by 3M.[15] Our ability to reversibly modulate the refractive indices presented to incoming light by both temperature and in future by applied electric field however, shows the possibility of fabricating switchable self-assembling polarizing filters. We have shown that we can achieve significant and reversible (~25 %) changes in the optical transmission of a 1D self-assembled alternating dielectric stack by using temperature changes to alter the refractive index contrast in the material via the isotropization of the LC mesophase in one of the stacks. Improvements over the current system would involve employing a material with a sharper isotropization transition for the hydrogen-bonded smectic mesophase, as well as utilizing a more thermally stable backbone to act as host. In addition, improved orientation of the layers and a much higher order parameter of the LC within the layers would lead to stronger and sharper optical responses and such materials are being pursued.

4. Experimental

A polystyrene-*block*-poly(*tert*-butylmethacrylate) (PS-*b*-TBMA) block copolymer was synthesized by sequential anionic polymerization in tetrahydrofuran (THF) at –78 °C under nitrogen using *sec*-butyl lithium as the initiator and anhydrous methanol for reaction termination. Hydrolysis of the PTBMA block was carried out by reaction with hydrochloric acid in 1,4-dioxane solution to give poly(methacrylic acid), PMAA. Molecular weight was characterized by gel permeation chromatography using a Waters instrument. The mesogenic additive was synthesized starting from 4,4′-biphenol. The structure of the mesogen and the diblock copolymer PS-*b*-MAA are given in Figure 2.

LC-BCP samples were prepared by solution blending varying amounts of the mesogen with the diblock copolymer at 2–5 wt.-% in THF. Solvent removal was conducted by evaporation over 18 h at RT (22–24 °C) in a THF vapor saturated atmosphere to produce films approximately 5 μm to 200 μm thick. Films were subsequently dried under vacuum for 12 h. The films were characterized thermally using differential scanning calorimetry (DSC) and optically, using polarized optical microscopy (POM) and transmission/reflectance spectrophotometry. Microstructures were observed using small-angle X-ray scattering (SAXS), and transmission electron microscopy (TEM). For TEM, thin sections were prepared using a Riechert-Jung ultramicrotome with dry pickup and imaged with a JEOL 2000FX instrument. Optical transmission spectra were taken as a function of temperature using a Linkham hot stage with a Zeiss Axioskop microscope.

[1] J. G. Fleming, S. Y. Lin, *Opt. Lett.* **1999**, *24*, 49.
[2] M. Campbell, D. N. Sharp, M. T. Harrison, R. G. Denning, A. J. Turberfield, *Nature* **2000**, *404*, 53.
[3] Y. Fink, J. N. Winn, S. H. Fan, C. P. Chen, J. Michel, J. D. Joannopoulos, E. L. Thomas, *Science* **1998**, *282*, 1679.
[4] S. A. Asher, J. Holtz, J. Weissman, G. S. Pan, *MRS Bull.* **1998**, *23*, 44.
[5] K. Lee, S. A. Asher, *J. Am. Chem. Soc.* **2000**, *122*, 9534.
[6] S. A. Asher, *Abstr. Pap. - Am. Chem. Soc.* **2001**, *221*, 15.
[7] Y. A. Vlasov, M. Deutsch, D. J. Norris, *Appl. Phys. Lett.* **2000**, *76*, 1627.
[8] J. F. Bertone, P. Jiang, K. S. Hwang, D. M. Mittleman, V. L. Colvin, *Phy. Rev. Lett.* **1999**, *83*, 300.
[9] Y. N. Xia, B. Gates, Y. D. Yin, Y. Lu, *Adv. Mater.* **2000**, *12*, 693.
[10] Y. N. Xia, *Adv. Mater.* **2001**, *13*, 369.
[11] Y. Fink, A. M. Urbas, M. G. Bawendi, J. D. Joannopoulos, E. L. Thomas, *J. Lightwave Technol.* **1999**, *17*, 1963.
[12] A. Urbas, R. Sharp, Y. Fink, E. L. Thomas, M. Xenidou, L. J. Fetters, *Adv. Mater.* **2000**, *12*, 812.
[13] A. C. Edrington, A. M. Urbas, P. DeRege, C. X. Chen, T. M. Swager, N. Hadjichristidis, M. Xenidou, L. J. Fetters, J. D. Joannopoulos, Y. Fink, E. L. Thomas, *Adv. Mater.* **2001**, *13*, 421.
[14] A. Urbas, Y. Fink, E. L. Thomas, *Macromolecules* **1999**, *32*, 4748.
[15] M. F. Weber, C. A. Stover, L. R. Gilbert, T. J. Nevitt, A. J. Ouderkirk, *Science* **2000**, *287*, 2451.
[16] J. M. Lehn, *Macromol. Symp.* **2001**, *174*, 5.
[17] M. Muthukumar, C. K. Ober, E. L. Thomas, *Science* **1997**, *277*, 1225.
[18] N. Susa, *Jpn. J. Appl. Phys., Part 1* **2000**, *39*, 6288.
[19] S. W. Leonard, J. P. Mondia, H. M. van Driel, O. Toader, S. John, K. Busch, A. Birner, U. Gosele, V. Lehmann, *Phys. Rev. B* **2000**, *61*, R2389.
[20] K. Busch, S. John, *Phys. Rev. Lett.* **1999**, *83*, 967.
[21] Y. K. Ha, Y. C. Yang, J. E. Kim, H. Y. Park, C. S. Kee, H. Lim, J. C. Lee, *Appl. Phys. Lett.* **2001**, *79*, 15.
[22] C. S. Kee, H. Lim, Y. K. Ha, J. E. Kim, H. Y. Park, *Phys. Rev. B* **2001**, *6408*, 5114.
[23] T. Kato, H. Kihara, S. Ujiie, T. Uryu, J. M. J. Frechet, *Macromolecules* **1996**, *29*, 8734.
[24] G. P. Mao, J. G. Wang, C. K. Ober, M. Brehmer, M. J. O'Rourke, E. L. Thomas, *Chem. Mater.* **1998**, *10*, 1538.
[25] D. W. Berreman, *J. Opt. Soc. Am. B* **1972**, *62*.
[26] C. O. Osuji, J. T. Chen, G. Mao, C. K. Ober, E. L. Thomas, *Polymer* **2000**, *41*, 8897.
[27] G. R. Mitchell, A. H. Windle, *Polymer* **1983**, *24*, 1513.